Carbohydrate Polymers 114 (2014) 424–431

Contents lists available at ScienceDirect

Carbohydrate Polymers

journal homepage: www.elsevier.com/locate/carbpol

Evaluation of reaction factors for deposition of silica (SiO_2) nanoparticles on cellulose fibers

Joabel Raabe[a,*], Alessandra de Souza Fonseca[a], Lina Bufalino[a], Caue Ribeiro[b], Maria Alice Martins[b], José Manoel Marconcini[b], Gustavo Henrique Denzin Tonoli[a]

[a] Department of Forest Science, Universidade Federal de Lavras, C.P. 3037, 37200-000 Lavras, MG, Brazil
[b] Laboratório Nacional de Nanotecnologia para o Agronegócio (LNNA), Embrapa Instrumentação, Caixa Postal 741, CEP 13560-970 São Carlos, SP, Brazil

ARTICLE INFO

Article history:
Received 29 January 2014
Received in revised form 22 July 2014
Accepted 8 August 2014
Available online 27 August 2014

Keywords:
Vegetable fibers
Cellulose treatment
Hybrid nanocomposites
Moisture adsorption

ABSTRACT

This study aimed to evaluate reaction conditions for deposition of SiO_2 nanoparticles on the surface of cellulose fibers and their influence on moisture adsorption of the hybrid organic–inorganic material formed. SiO_2 nanoparticle deposition was carried out with the sol–gel process testing four reaction times (2, 12, 18, and 24 h) and three contents of the tetraethyl-orthosilicate (TEOS) precursor (1.9, 4.2 and 8.4 g g^{-1} of cellulose fiber). Modification time and TEOS content directly influence the amount of Si deposited on the fiber surface, nanoparticle diameter distribution, thermal stability, and resistance to moisture adsorption. There is a tendency of slight increase of nanoparticle size and the amount of Si deposited with increasing reaction time. SiO_2 nanoparticles were bonded on the surface of the cellulose fibers and are able to improve thermal stability of the material, increasing onset degradation temperature. The moisture adsorption capacity of the modified cellulose fiber was reduced up to 50%.

1. Introduction

Cellulose fibers from wood and annual crops are widely available in most developing countries. They provide several advantages in comparison to synthetic fibers, such as low density, renewability, variety of sources and properties, and low cost. Natural fibers are hence suitable to be used as reinforcement in polymeric and cement matrices as often proved in the literature (Belgacem & Gandini, 2008; Böer, Holliday, & Kang, 2014; Sabu & Pothan, 2008; Savastano, John, Agopyan, & Moslemi, 2010). However, the main disadvantages of using those fibers as reinforcements are: (i) dimensional instability due to high hydrophilic nature of the cellulose fibers, which easily adsorbs water from the environment (Tonoli et al., 2013); and (ii) chemical incompatibility with most polymeric matrices, which results in poor stress transference in the fiber–matrix interface (Doan, Gao, & Mader, 2006; Kabir, Wang, Lau, & Cardona, 2012; Campos et al., 2012). Modifications of the fiber surface and structural properties by physical and chemical processes are mainly based on the reactivity of the cellulose hydroxyls, and may be an interesting alternative to improve fiber water resistance (Faruk, Bledzki, Fink, & Sain, 2012; Kabir et al., 2012; Kalia, Kaith, & Kaur, 2009; Liu, Xie, Yu, Chena, & Li, 2009; Skreekumar, Kuruvilla, Unnikrishnan, & Sabu, 2011).

Hybrid organic–inorganic materials may be produced by nanoparticle deposition on the fiber surface. Those treatments aim to decrease water adsorption, by reducing the amount of free hydroxyl groups, and to improve mechanical properties of the hybrid material and of the ensuing composites (Ashori, Sheykhnazari, Tabarsa, Shakeri, & Golalipour, 2012; Pinto, Marques, Barros-Timmons, Trindade, & Pascoal Neto, 2008; Shi, Lu, Guo, Zhang, & Cao, 2013). The sol–gel process is one of the main methodologies to modify cellulose fibers with inorganic materials. This process is based on hydrolysis and condensation reaction (in situ) of the inorganic precursor on an organic surface (Pinto et al., 2008). It allows strong chemical interactions to be formed, besides keeping the precursor properties (Sanchez, Julián, Belleville, & Popall, 2005). The synergy effect of the process generates materials with new properties and potential applications. For instance, increased mechanical strength and fire resistance may be achieved, as much as additional hydrophobic or antifogging features, allowing the hybrid materials to be applied as scratch-resistant coatings. Furthermore, The enhancement of mechanical and thermal properties of polymers by the addition of inorganic properties offers the possibility for these fibers to substitute classical compounds based on

* Corresponding author. Tel.: +55 35 3829 1411; fax: +55 35 3829 1411.
E-mail address: joabeljr@hotmail.com (J. Raabe).

http://dx.doi.org/10.1016/j.carbpol.2014.08.042
0144-8617/

metals and ceramics, or as fire retardant materials for construction and packing industry (Balazs, Emrick, & Russell, 2006; Caseri, 2007; Krishnamoorti & Vaia, 2007; Schadler, Kuar, Benicewicz, Lewis, & Harton, 2007; Schaefer & Justice, 2007).

Factors such as the water/precursor proportion (molar ratio), the use of any type of catalyst (acid or alkaline), the temperature of reaction and the solvent type, strongly influence the kinetic reaction and the structure and morphology of the new material formed by the sol–gel process (Tripathi & Shahi, 2011). However, there is a lack of information about the influence of the reaction factors (reaction time and precursor concentration) on the size distribution of the nanoparticles obtained, on the thermal properties and on the moisture adsorption of the hybrid (cellulose + SiO_2) material formed.

Therefore, this study aimed to evaluate the effect of the synthesis variables (reaction time and precursor content) for the surface modification of cellulose fibers by the sol–gel process, through the in situ synthesis of SiO_2 nanoparticles chemically bonded to the fiber surface.

Effectiveness of fiber modification was evaluated by thermal and moisture adsorption analyses of the hybrid organic–inorganic materials obtained in order to find the best process conditions.

2. Methodology

2.1. Material

Eucalyptus (hybrid: *Eucalyptus urophylla* × *Eucalyptus grandis*) cellulose fibers were obtained from the commercial Kraft pulping process, with average fiber length of 0.81 ± 0.01 mm and average width of 15.9 ± 0.3 μm. Chemical composition of the fibers was cellulose (86.3%), hemicelluloses (12.9%), ashes and extractives (0.8%).

Chemicals include the inorganic SiO_2 precursor tetraethyl orthosilicate ($C_8H_{20}O_4Si$ – TEOS, 98%), the synthesis catalyst ammonium hydroxide (NH_4OH – 30% v v^{-1}), the ethanol solvent (CH_3CH_2OH – 95% P.A.), and the potassium sulfate (K_2SO_4) used for humidity control in the moisture adsorption test.

2.2. Deposition of the SiO_2 nanoparticles on the cellulose fibers

Cellulose fibers were kept in deionized water under mechanical stirring during 24 h in order to achieve total disintegration of the cellulose pulp sheets and proper fiber dispersion. Water to fiber consistency for this dispersion was 100 mL g^{-1}.

Modification of the cellulose fibers with the deposition of the SiO_2 nanoparticles was carried out by the sol–gel process, based on previous studies (Ashori et al., 2012; Pinto et al., 2008). 0.5 g of cellulose fibers was immersed in a solution composed of 42.5 mL of ethanol, 4.5 mL of deionized water, and 0.75 mL of ammonium hydroxide. Constant and moderate mechanical stirring (300 rpm) was kept for 2 h, after which TEOS solution was slowly added drop-by-drop and a solution with fiber consistency of 100 mL g^{-1} was achieved. Four reaction times (2, 12, 18 and 24 h) and three TEOS contents (1.9, 4.2 and 8.4 g of TEOS per g of cellulose pulp fiber) were tested (Table 1). All modifications were performed at room conditions (around 25 °C and 70% RH).

The resultant modified fibers were vacuum filtered and thoroughly washed with deionized water until the filtered water becomes clean. The modified fibers were conditioned between filter paper sheets and kept in a desiccator during 24 h. Afterwards, the modified fibers were pressed under 3.3 MPa for 5 min in order to obtain a fiber sheet with flat surface. The fiber sheets were dried at 60 °C for 48 h before characterization.

Table 1
Fiber modification conditions.

Samples	Time of reaction (h)	TEOS content (g g^{-1})
Control	–	–
$T_2C_{1.9}$	2	1.9
$T_2C_{4.2}$		4.2
$T_2C_{8.4}$		8.4
$T_{12}C_{1.9}$	12	1.9
$T_{12}C_{4.2}$		4.2
$T_{12}C_{8.4}$		8.4
$T_{18}C_{1.9}$	18	1.9
$T_{18}C_{4.2}$		4.2
$T_{18}C_{8.4}$		8.4
$T_{24}C_{1.9}$	24	1.9
$T_{24}C_{4.2}$		4.2
$T_{24}C_{8.4}$		8.4

2.3. Scanning electron microscopy (SEM)

Morphological characteristics of the fibers were evaluated by SEM micrographs in a JEOL JSM-6510 microscope with a tungsten filament operating at 15 kV. An energy dispersive spectroscopy (EDS) system (model JEOL 6742A – Ultradry Silicon Drift) with an active area of 10 mm^2 and 132 eV resolution was used to detect and semi-quantification of SiO_2 particles at the fiber surface. Average percentage of Si (% by mass) was obtained after five scans per sample in a 1 μm^2 area. The fiber samples were bonded over a carbon tape on the metallic stubs and carbon coated (for EDS measurements) and gold coated (for MEV observations) before analyses.

Measurements of the SiO_2 nanoparticle diameters were performed using the Image J software, as reported in Mori et al. (2014). About 100 measurements were recorded for each condition in the SEM representative images, in order to obtain the diameter distribution of the nanoparticles at the cellulose fiber surface. The average diameter values were submitted to variance analysis and the averages were compared among reaction times and precursor content by Tukey test at 5%.

2.4. Fourier transform infrared (FTIR) spectroscopy

FTIR spectrum of the samples was recorded with a FTIR Perkin Elmer (Spectrum 1000) equipped with Spectrum v5-3.1 software to compare the chemical structure of unmodified and modified cellulose fibers. The samples were milled into powders with KBr at a proportion of 1:100 (w:w), and pressed to form the sample disks. Sixteen scans were performed in the spectral range of 400–4000 cm^{-1} with 1 cm^{-1} resolution at the transmittance mode.

2.5. Thermogravimetric analysis (TGA)

Raw and modified fibers were subject to thermogravimetric analysis (TGA) in a TA Instruments analyzer (model Q500) as proposed in Tonoli et al. (2012). The samples with around 7 mg were heated in a Pt crucible from 25 to 600 °C in synthetic air flowing at 60 mL min^{-1}, and heating rate of 10 °C min^{-1}.

2.6. Moisture adsorption analysis

Three samples of each modification condition (2.0 cm × 1.0 cm × 0.1 cm) were pre-dried overnight at 105 °C, weighted and placed in hermetically closed containers with 97 ± 2% of relative humidity (RH) and 20 ± 2 °C, using a saturated potassium sulfate solution, as prescribed by the ASTM E104 (2012) standard. The moisture adsorbed by the samples along the time was determined by weighting (0.0001 g precision) them at

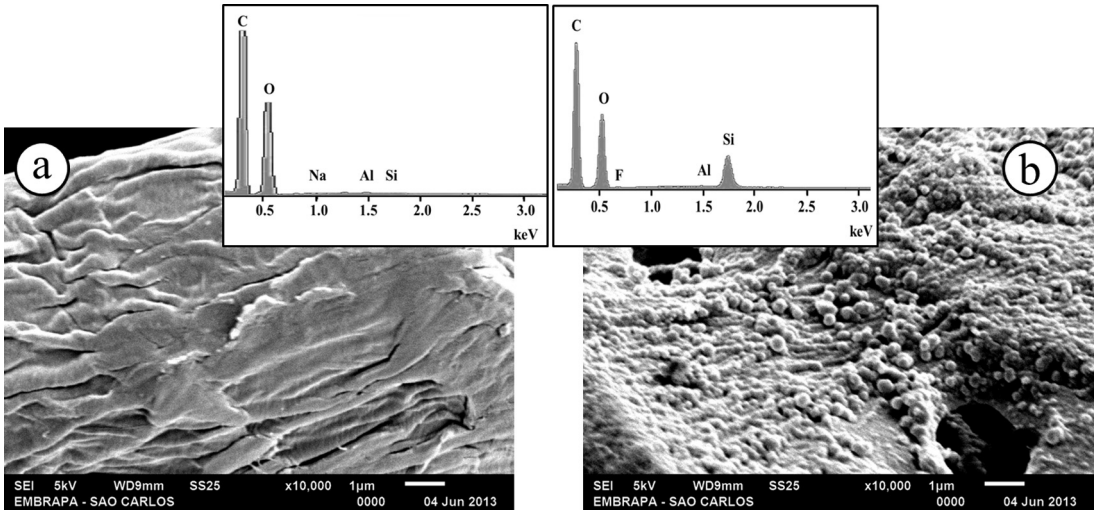

Fig. 1. SEM images and EDS measurements of: (a) unmodified and (b) modified cellulose fibers ($T_{12}C_{4.2}$).

successive intervals until they reached a constant weight. The amount of moisture adsorbed (MA) by the samples was calculated as follows (Eq. (1)):

$$MA(\%) = \left[\frac{M_t - M_0}{M_0}\right] \times 100 \quad (1)$$

where M_0 and M_t are the initial mass of the sample (prior to exposure to moisture) and the sample mass after t hours of exposure to moisture (97 ± 2% RH), respectively. Each data point represents an average of three samples.

3. Results and discussion

3.1. Morphology of the SiO_2 nanoparticles on the cellulose fibers

Raw cellulose fibers presented smooth and uniform surface, basically comprised of carbon (C) and oxygen (O), with small and negligible amounts of sodium (Na), aluminum (Al) and silicon (Si) and a characteristic Si peak (Fig. 1a).

SEM and EDS analyses of the modified fibers (Fig. 1b) show the SiO_2 nanoparticles deposited on the fiber surface, as observed by the increase of the Si peak in the EDS measurement, which proves the effective modification with SiO_2 nanoparticles well dispersed at the fiber surface. This SiO_2 deposition is caused by the hydrolysis of the TEOS precursor and subsequent condensation of the resultant hydroxyls groups on the surface of the fibers (Tripathi & Shahi, 2011; Xie, Yu, & Shi, 2009). Although no information is available from EDS measurements about the thickness or degree of SiO_2 covering, the results strongly suggest that a hybrid cellulose + SiO_2 composite was formed, since Si peak was remarkably intense in relation to C and O peaks (Tonoli et al., 2009). Other studies showed successful modification of cellulose fibers with TEOS precursor by the sol–gel process. Properties achieved include reduction on water uptake and improvement of mechanical strength due to strong chemical interactions between cellulose and silica phases (Ashori et al., 2012; Pinto et al., 2008). On the other hand, further studies are needed to verify if the high silica content on the modified fibers causes excessive tool wear during processing. For example, researchers reported concerns on this matter for application of bamboo as composite lumber (Malanit, Barbu & Früwald, 2007), black locus wood species for particleboard production (Nemli et al., 2004), and rice and bamboo for MDF production (Hiziroglu, Bauchongkol, Fueangvivat, Soontonbura, & Jarusombuti, 2007).

Table 2
Average diameter (in nm) and standard deviation of the SiO_2 particles deposited on the fiber surface.

Conditions	$C_{1.9}$	$C_{4.2}$	$C_{8.4}$	Fc
T_2	149 ± 35 a A[a]	160 ± 58 c A	147 ± 49 b A	1.467[ns]
T_{12}	131 ± 37 b B	166 ± 55 c A	178 ± 50 a A	18.901[*]
T_{18}	158 ± 35 a B	192 ± 45 b A	147 ± 47 b B	19.890[*]
T_{24}	165 ± 54 a B	271 ± 52 a A	161 ± 45 ab B	92.024[*]
Fc	8.567[ns]	60.801[*]	6.621[*]	–

[*] Fc: calculated F, significant at 5%.
[a] Averages followed by the same letter do not differ according to Tukey test.
[ns] non-significant at 5%; small and capital letters compare reaction times and precursor contents respectively.

Fig. 2 shows semi-quantitative data (from EDS measurements) of the Si content (by mass) deposited on the cellulose fibers under different reaction conditions. The Si content of all the modified fibers was far higher in relation to control sample. No remarkable increase in the average Si content was observed when modification time varied from 2 to 18 h, but a higher percentage of Si deposited was observed after 24 h of reaction. In general, 4.2 g g^{-1} of TEOS was the most efficient level for adhering SiO_2 on fiber surface.

SEM micrographs of the modified fibers were used in order to investigate the diameter of the SiO2 particles deposited on the fiber surface (Table 2). Average particle diameter was over 100 nm for all modification conditions. The lowest (131 ± 37 nm) and highest average diameter values (271 ± 52 nm) were found for $T_{12}C_{1.9}$ and $T_{24}C_{4.2}$, respectively. This result may be attributed to the water:precursor ratio close to 1 for higher TEOS content. The water:precursor ratio is one of the main factors that influence the kinetics of hydrolysis and poly-condensation reactions (Tripathi & Shahi, 2011). Higher SiO_2 particle diameters will result in cellulose fiber with greater recovering, while lower SiO_2 spread particles will provide greater superficial area for the fibers. A clear increase of particle diameter with increase in reaction time was observed for the TEOS content of 4.2 g g^{-1} ($C_{4.2}$). For reaction times of 18 and 24 h, the concentration of 4.2 g g^{-1} of TEOS resulted in the higher diameter values of the particles. For 12 h of reaction (T_{12}) the lower value of particle diameter was observed for 1.9 ($C_{1.9}$). There was no significant difference among averages from different precursor contents for 2 h of reaction (T_2 series). Increase in diameter with increase in precursor content from $C_{1.9}$ to $C_{4.2}$ was observed for 12 (T_{12}), 18 (T_{18}) and 24 h (T_{24}), but the values significant decrease when 8.4 g g^{-1} ($C_{8.4}$) content was used for longer reaction times.

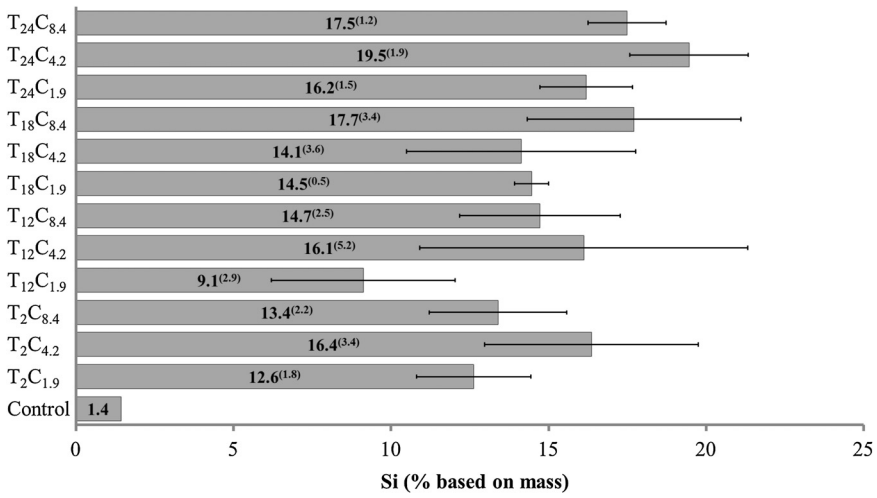

Fig. 2. Average values and standard deviation (in parenthesis) of the content of Si (by mass) deposited on the fiber surface.

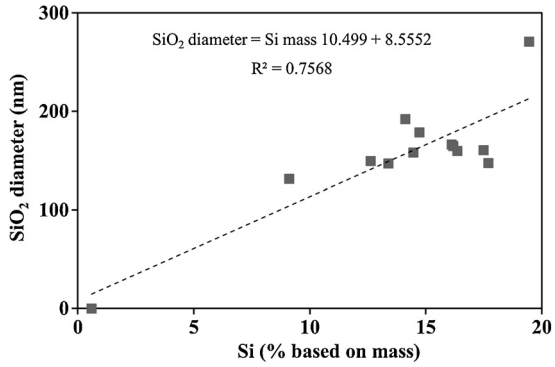

Fig. 3. Relation between average SiO_2 diameter (nm) of the nanoparticles and the content of Si (% by mass) determined by EDS measurements on the fiber surface.

Fig. 3 shows the linear relation ($R^2 = 0.76$) between average diameter of the SiO_2 nanoparticles and Si content (by mass) deposited on the cellulose fiber surface. This result may allow predicting SiO_2 particle diameter, based on the content of Si (measured by EDS semi-quantification) deposited on the fiber surface, if the modification conditions proposed in this work are kept the same. The TEOS content of 4.2 g g^{-1} resulted in the highest Si content (by mass) deposited and higher average diameter of the SiO_2 nanoparticle for all reaction times. The accumulated frequency of the SiO_2 nanoparticle diameter deposited on the fiber surface was determined in order to verify the effect of modification conditions on the diameter distribution of the nanoparticles (Fig. 4). The TEOS content of 8.4 g g^{-1} resulted in the higher amount of particles (around 70%) with diameter values below 150 nm, which in turn may provide higher surface area. Higher TEOS content (8.4 g g^{-1})

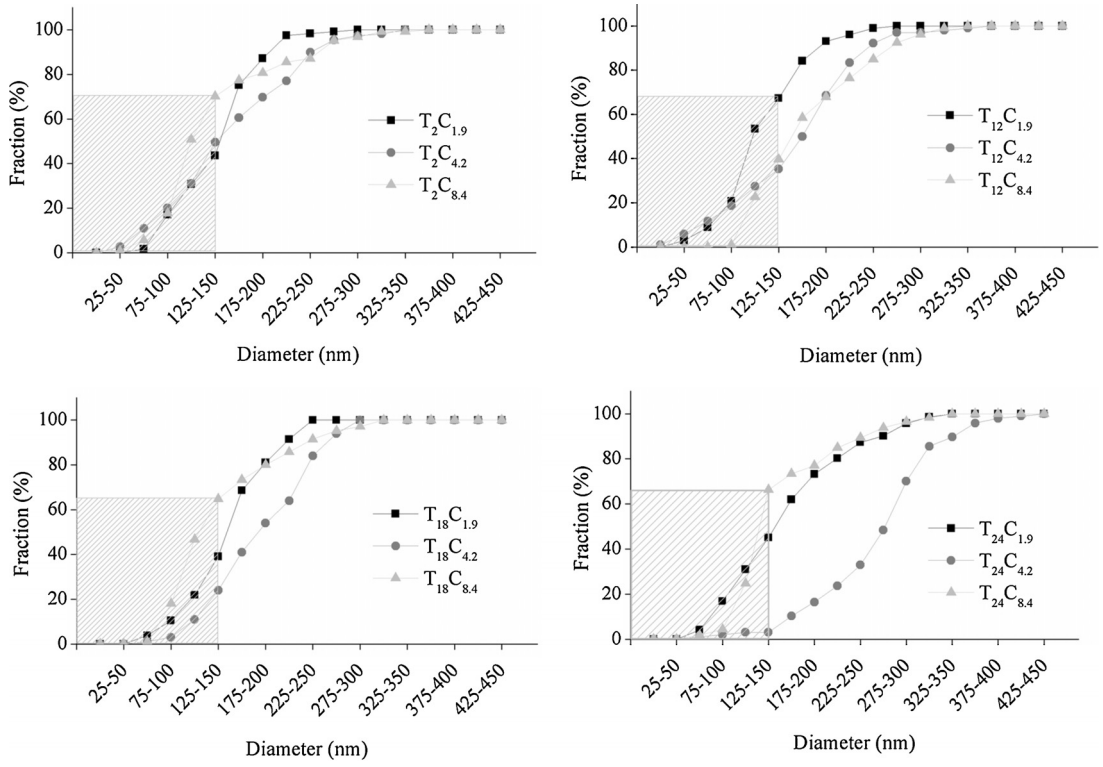

Fig. 4. Accumulated diameter distribution of SiO_2 nanoparticles deposited on the fiber surface.

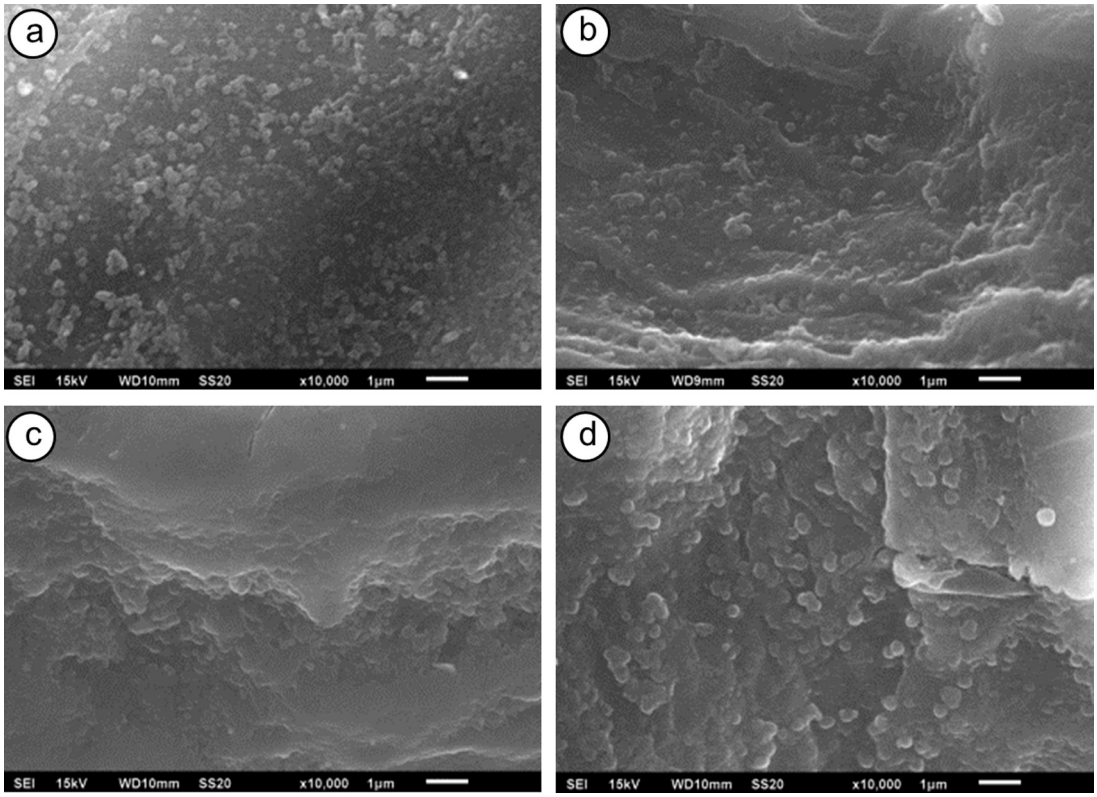

Fig. 5. SEM analysis of modified fibers from conditions (a) $T_2C_{1.9}$, (b) $T_{12}C_{1.9}$, (c) $T_{18}C_{8.4}$ and (d) $T_{24}C_{4.2}$.

seems to provide more stable nanoparticles in the first hours of reaction, and thus longer reaction times (18 and 24 h) did not increase the nanoparticle size, but maintain the content of lower-size particles. Probably, in the lower concentrations, the higher water:precursor ratio lead to agglomeration of the inorganic particles, which increased the nanoparticle size with the increase in the reaction time. An exception is observed for 12 h of time reaction, whose higher amount of particles with lower diameter was obtained for the concentration of 1.9 g g^{-1}. This result shows that particle size depends on TEOS concentration and time of reaction, which may be important in future studies on fiber modification destined to composite reinforcement.

The SEM images (Fig. 5) show the dispersion of the SiO_2 particles on the surface of the cellulose fibers treated under different conditions. The images were selected on the basis of morphological differences found between the modified fibers. The SiO_2 nanoparticles were clearly observed in the samples $T_2C_{1.9}$ (Fig. 5a) and $T_{12}C_{1.9}$ (Fig. 5b), probably due to the lower content of Si deposited onto the fibers (Fig. 2), which led to good dispersion and individualized particles at the fiber surface. The nanoparticles produced under these conditions ($T_2C_{1.9}$ and $T_{12}C_{1.9}$) are lower in diameter than in the sample $T_{24}C_{4.2}$ (Fig. 5d). The fibers treated under the condition $T_{18}C_{8.4}$ seems to present a uniform coating layer, with almost no space between the deposited nanoparticles (Fig. 5c).

3.2. FTIR results

The typical FTIR spectra obtained for unmodified and modified ($T_{18}C_{8.4}$) fibers are depicted in Fig. 6. The FTIR spectra for the other conditions of fiber modification feature the same profile as the spectra shown in Fig. 6b, however with a small variation in the intensity of the peaks. In this case, it was used the $T_{18}C_{8.4}$ condition as the typical condition to show the structural modification occurred on the fiber. Both spectra presented a wide band in the region between

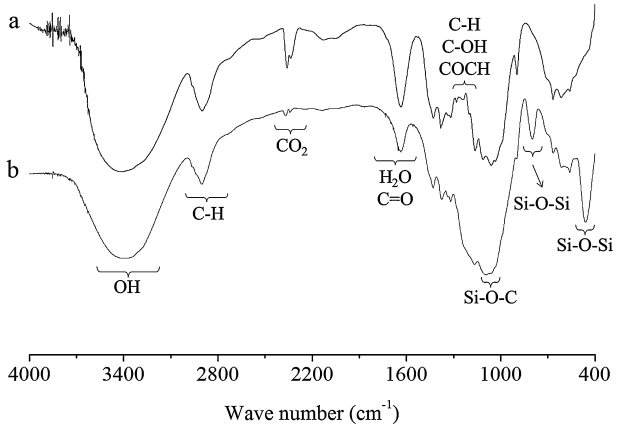

Fig. 6. FTIR spectra of: (a) unmodified; and (b) modified ($T_{18}C_{8.4}$) fibers.

3600 and 3200 cm^{-1}, which is characteristic from vibrations of the OH groups present in the cellulose molecules (Ashori et al., 2012; Lu et al., 2013). The 2903 cm^{-1} band is related to stretching of aliphatic C—H from methyl groups (Sinha & Rout, 2008). The peak between 1800 and 1600 cm^{-1} may be related to both stretching of C=O from carbonyl groups found in hemicelluloses (Pires, Merlini, Al-Qureshi, Salmória, & Barra, 2012) or water adsorption in cellulose fibers (peak at 1635 cm^{-1}). The peak at 1635 cm^{-1} related to water adsorption of the fibers (Ashori et al., 2012) was remarkably reduced with fiber modification (Fig. 6b). This result may be mainly attributed to the reduction of the hydrophilic character provided by the silica nanoparticles. The bands between 1350 and 1150 cm^{-1} presented peaks related to deformations of C—OH, C—H and C—O—C groups of cellulose and hemicelluloses (Ashori et al., 2012; Pires et al., 2012). Changes in this region may be related to hemicelluloses removal since they are partially solubilized at

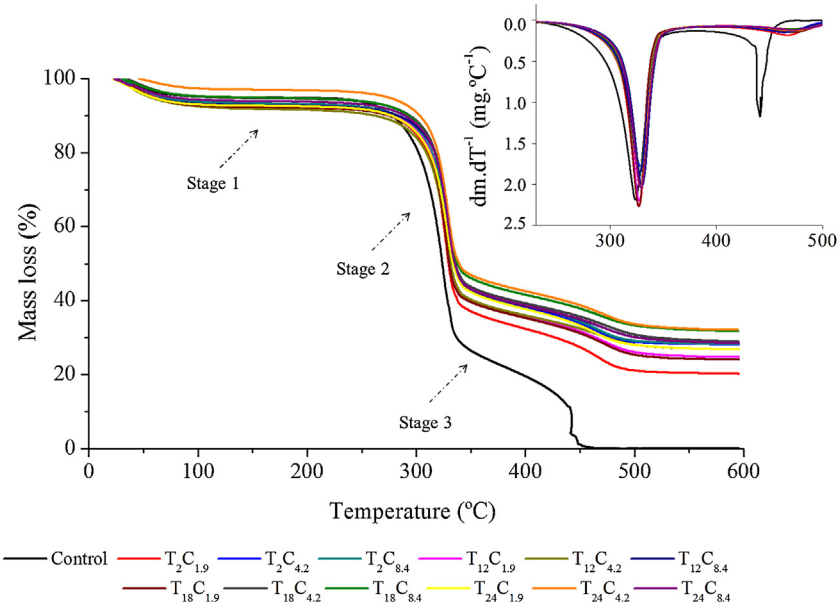

Fig. 7. TG and DTG (detail) curves and degradation stages of unmodified and modified fibers.

low alkali concentrations used in the present reaction condition (Corrales et al., 2007).

The FTIR spectra of the modified fibers (Fig. 6b) shows the three main typical silica bands detectable in the regions near to 450 cm^{-1}, 800 cm^{-1} and 1100 cm^{-1}, which are attributed to stretching vibration of Si—O—Si, Si—O—Si and Si—O—C, respectively (Lu et al., 2013; Naghsh, Sadeghi, Moheb, Chenar, & Mohagheghian, 2012). The presence of those peaks (at 450 cm^{-1}, 800 cm^{-1} and 1100 cm^{-1}) strongly suggests that chemical bonding between cellulose and silica was formed after superficial modification (Ashori et al., 2012; Machado et al., 2011; Nassar et al., 2007; Shi et al., 2013).

3.3. Thermal properties

Thermogravimetric (TG) curves of the unmodified and modified cellulose fibers are presented in Fig. 7. Thermal properties of the cellulose fibers should be investigated when it is important to evaluate their potential as reinforcement in thermoplastic polymers that processing requires temperatures above 200 °C. Also, this property can reveal the nanoparticle–fiber interaction, since dislocations in thermal events are expected if novel strong bondings are present. For all modifying conditions, thermal decomposition occurs in three stages. The first one ranges between room temperature and 150 °C and it is related to sample dehydration (Yildiz & Gumuskaya, 2007) and volatile releases (Beg & Pickering, 2008). Mass loss related to dehydration varies between 3 and 8%. The second stage is related to decomposition of the fiber structure. Hemicelluloses present amorphous structure and, hence are the first components to degrade (at around 160 °C), while cellulose decomposes between 225 and 370 °C (Órfão, Antunes, & Figueiredo, 1999). The highest mass loss (50–70%) occurred in this second stage, whose the temperature decomposition ranges between 200 and 340 °C, depending on the modification condition. The third stage of decomposition occurs between 340 and 500 °C due to oxidation of remaining organic material. In some cases the thermal degradation steps are not so easily identified/isolated, because of the complexity of degradation reactions (Corradini, Imam, Agnalli, & Mattoso, 2009).

Results from thermal analysis indicate that deposition of the SiO_2 nanoparticles contributes to improve thermal stability of the cellulose fibers, since increased the onset degradation temperature (detail in the DTG curves of Fig. 7). Furthermore, the high mass loss ratio (detail in the stage 2 of Fig. 7) was slightly in lower temperatures in unmodified fibers. The higher the content of SiO_2 nanoparticles, the higher was the thermal stability. The remaining waste in the modified fibers at 600 °C varied from 20.2% (for $T_2C_{1.9}$) to 32.1% (for $T_{24}C_{4.2}$), corroborating with the behavior observed in the EDS measurements of the Si content (Fig. 2). Those values are far higher than the value found for unmodified fiber (around 1% of residual mass) and are certainly related to the Si inorganic species adhered to the organic fibers.

3.4. Moisture adsorption

Most samples had their mass gain stabilized after 288 h of exposition to controlled humidity. After mass stabilization was reached, unmodified fibers showed remarkable higher moisture adsorption (25.0 ± 0.5%) in relation to modified fibers. Only cellulose fibers modified by $T_{12}C_{4.2}$, $T_{12}C_{8.4}$, $T_{24}C_{1.9}$ and $T_{24}C_{4.2}$ conditions have reached the mass stabilization after 384 h, while $T_{18}C_{4.2}$ and $T_{18}C_{8.4}$ samples achieved the stability of the moisture adsorption after 480 h. Deposition of SiO_2 nanoparticles has decreased the hydrophilic character of the cellulose fibers. Nevertheless, the results did not show a clear relation between time reaction and moisture adsorption of the fibers (Fig. 8). This result may be partially attributed to heterogeneity in diameter and distribution of SiO_2 particles in the different modification conditions, which directly influences hydrophilic capacity of the fibers. Fibers modified using 18 h of reaction presented the lower moisture adsorption (between 12.3% and 13.0%), which corroborate with the finding reported in the previous sections where the fibers modified under the $T_{18}C_{8.4}$ condition presented a uniform SiO_2 coating layer on the fiber surface, when compared to their counterparts. Furthermore, increasing the TEOS content seems to decrease moisture adsorption, as expected due to the decrease of the free hydroxyls available at the fiber surface when SiO_2 particles are present.

Apart from improving thermal and moisture adsorption properties, it is expected that deposition of SiO_2 particles on cellulose fiber surface improve the dispersion of the cellulose fibers when applied as composite reinforcement in apolar matrices (Felix & Gatenholm, 1991). This is because the reduction of the free hydroxyl groups available at the fiber surface, decreases the strong interactions

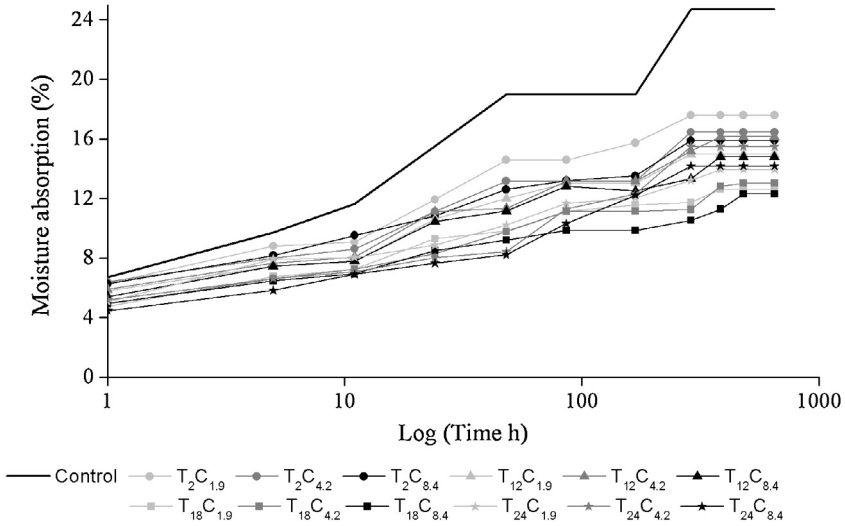

Fig. 8. Moisture adsorption of unmodified and modified fibers.

between fibers (Hubbe, Venditti, & Rojas, 2007). Other benefits from using these modified fibers include the improvements in dimensional stability of the fibers, and the increase in the fiber surface area. As a result, increases in the interaction between composite phases may lead to the improvement of the mechanical strength (Mathew, Oksman, & Sain, 2005). These results can be interesting for ongoing research in the direction of fiber modification strategies for application of the cellulose fibers as durable reinforcement in different advanced composites.

4. Conclusions

Surface modification of cellulose fibers by SiO_2 nanoparticle deposition was successfully achieved for all conditions proposed in this study. Modification time and TEOS precursor content directly influence the amount of Si deposited on the fiber surface, the nanoparticle diameter distribution, the fiber thermal stability, and resistance to moisture adsorption. There is a tendency of increase of nanoparticle size and the amount of Si deposited with increasing reaction time. SiO_2 nanoparticles were chemically bonded on the surface of the cellulose fibers and were able to improve the thermal stability of these fibers. It was observed a reduction of up to 50% in the moisture adsorption capacity of the modified cellulose fibers. The present study contributes to the widespread use of the cellulose fibers and with information for understanding the major mechanisms that influence the mechanical and physical performance of cellulose based materials. The fiber modification used here led to distinct morphological and structural characteristics of the cellulose fiber, which can be used to engineer polymeric composites for multipurpose applications, e.g. in the construction or packing industry.

Acknowledgements

Financial support for this research project was provided by the Conselho Nacional de Desenvolvimento Científico e Tecnológico (CNPq), Fundação de Amparo à Pesquisa do Estado de São Paulo (Fapesp), Fundação de Amparo à Pesquisa do Estado de Minas Gerais (Fapemig), Coordenação de Aperfeiçoamento de Pessoa de Nível Superior (Capes) and Empresa Brasileira de Pesquisa Agropecuária (Embrapa), Capes-Embrapa program, in Brazil. Thanks also to Rede Brasileira de Compoísitos e Nanocompoísitos Lignoceluloísicos (Religar).

References

Ashori, A., Sheykhnazari, S., Tabarsa, T., Shakeri, A., & Golalipour, M. (2012). Bacterial cellulose/silica nanocomposites: Preparation and characterization. *Carbohydrate Polymers*, *90*, 413–418.

Balazs, A. C., Emrick, T., & Russell, T. P. (2006). Nanoparticle polymer composites: Where two small worlds meet. *Science*, *314*, 1107–1110.

Beg, M. D. H., & Pickering, K. L. (2008). Accelerated of unbleached and bleached Kraft wood fibre reinforced polypropylene composites. *Polymer Degradation and Stability*, *93*, 1939–1946.

Belgacem, M. N., & Gandini, A. (Eds.). (2008). *Monomers, polymers and composites from renewable resources*. Amsterdam: Elsevier.

Böer, P., Holliday, L., & Kang, T. H. K. (2014). Interaction of environmental factors on fiber-reinforced polymer composites and their inspection and maintenance: A review. *Construction and Building Materials*, *50*(15), 209–218.

Campos, A., Tonoli, G. H. D., Marconcini, J. M., Mattoso, L. H. C., Klamczynski, A., Gregorski, K. S., et al. (2012). TPS/PCL composite reinforced with treated sisal fibers: Property, biodegradation and water-absorption. *Journal of Polymers and the Environment*, *21*, 1–7.

Caseri, W. (2007). Nanocomposites of polymers and inorganic particles. In G. Kickelbick (Ed.), *Hybrid materials. Synthesis, characterization, and applications* (pp. 49–83). Weinheim, Germany: Wiley-VCH.

Corradini, E., Imam, S. H., Agnalli, J. A. M., & Mattoso, L. H. C. (2009). Effect of coconut, sisal and jute fibers on the properties of starch/gluten/glycerol matrix. *Journal of Polymers and Environment*, *17*, 1–9.

Corrales, F., Vilaseca, F., Llop, M., Gironès, J., Mendéz, J. A., & Mutjé, P. J. (2007). Chemical modification of jute fibers for the production of green-composites. *Journal of Hazardous Materials*, *144*, 730–737.

Doan, T. T. L., Gao, S. L., & Mader, E. (2006). Jute/polypropylene composites I. Effect of matrix modification. *Composites Science and Technology*, *66*(7–8), 952–963.

Faruk, O., Bledzki, A. K., Fink, H. P., & Sain, M. (2012). Biocomposites reinforced with natural fibers: 2000–2010. *Progress in Polymer Science*, *37*, 1552–1596.

Felix, J. M., & Gatenholm, P. (1991). The nature of adhesion in composites of modified cellulose fibers and polypropylene. *Journal of Applied Polymer Science*, *42*(3), 609–620.

Hiziroglu, S., Bauchongkol, P., Fueangvivat, V., Soontonbura, W., & Jarusombuti, S. (2007). Selected properties of medium density fiberboard (MDF) panels made from bamboo and rice straw. *Forest Products Journal*, *57*(6), 46–50.

Hubbe, M. A., Venditti, R. A., & Rojas, O. J. (2007). What happens to cellulosic fibers during papermaking and recycling? A review. *BioResource*, *2*(4), 739–788.

Kabir, M. M., Wang, H., Lau, K. T., & Cardona, F. (2012). Chemical treatments on plant-based natural fibre reinforced polymer composites: An overview. *Composites: Part B*, *43*(7), 2883–2892.

Kalia, S., Kaith, B. S., & Kaur, I. (2009). Pretreatments of natural fibers and their application as reinforcing material in polymer composites? *Polymer Engineering & Science*, *49*(7), 1253–1272.

Krishnamoorti, R., & Vaia, R. A. (2007). Polymer nanocomposites. *Journal of Polymer Science, Part B: Polymer Physics*, *45*, 3252–3256.

Liu, H., Xie, F., Yu, L., Chena, L., & Li, L. (2009). Thermal processing of starch-based polymers. *Progress in Polymer Science*, *34*, 1348–1368.

Lu, T., Jiang, M., Jiang, Z., Hui, D., Wang, Z., & Zhou, Z. (2013). Effect of surface modification of bamboo cellulose fibers on mechanical properties of cellulose/epoxy composites. *Composites: Part B*, *51*, 28–34.

Machado, J. K. F. B., Marçal, A. L., Lima, O. J., Ciuffi, K. J., Nassar, E. J., & Calefi, P. S. (2011). Materiais híbridos orgânico-inorgânicos (ormosil) obtidos por sol-gel com potencial uso como filtro solar. *Química Nova*, *34*(6), 945–949.

Malanit, P., Barbu, M. C., & Früwald, A. (2007). The glutability and bonding quality of an Asian bamboo (*Dendrocalamus asper*) for the production of composite lumber. *Journal of Tropical Forest Science*, *21*(4), 361–368.

Mathew, A. P., Oksman, K., & Sain, M. (2005). Mechanical properties of biodegradable composites from poly lactic acid (PLA) and microcrystalline cellulose (MCC). *Journal of Applied Polymer Science*, *97*, 2014–2025.

Mori, C. L. S. O., Passos, N. A., Oliveira, J. E., Mattoso, L. H. C., Mori, F. A., Carvalho, A. G., et al. (2014). Electrospinning of zein/tannin bio-nanofibers. *Industrial Crops and Products*, *52*, 298–304.

Naghsh, M., Sadeghi, M., Moheb, A., Chenar, M. P., & Mohagheghian, M. (2012). Separation of ethylene/ethane and propylene/propane by cellulose acetate–silica nanocomposite membranes. *Journal of Membrane Science*, *423–424*, 97–106.

Nassar, E. J., Ávila, L. R., Perreira, P. F. S., Nassor, E. C. O., Cestari, A., Ciuffi, K. J., et al. (2007). Fenilsilicato dopado com Eu III obtido pelo método sol-gel. *Química Nova*, *30*(7), 1567–1572.

Nemli, G., Hiziroglu, S., Usta, M., Serin, Z., Ozdemir, T., & Kalaycioglu, H. (2004). Effect of residue type and tannin content on the properties of particleboard manufactured from black locust. *Forest Products Journal*, *54*(2), 36–40.

Órfão, J. J. M., Antunes, F. J. A., & Figueiredo, J. L. (1999). Pyrolysis kinetics of lignocellulosic materials-three independent reaction models. *Fuel*, *78*(3), 349–358.

Pinto, R. J. B., Marques, P. A. A. P., Barros-Timmons, A. M., Trindade, T., & Pascoal Neto, C. (2008). Novel SiO_2/cellulose nanocomposites obtained by in situ synthesis and via polyelectrolytes assembly. *Composites Science and Technology*, *68*, 1088–1093.

Pires, E. N., Merlini, C., Al-Qureshi, H. A., Salmória, G. V., & Barra, G. M. O. (2012). Efeito do tratamento alcalino de fibras de juta no comportamento mecânico de compósitos de matriz epóxi. *Polímeros*, *22*(4), 339–344.

Sabu, T., & Pothan, L. (2008). *Cellulose fibre reinforced polymer composites*. Philadelphia: Old City Publishing.

Sanchez, C., Julián, B., Belleville, P., & Popall, M. (2005). Applications of hybrid organic–inorganic nanocomposites. *Journal of Materials Chemistry*, *15*, 3559–3592.

Savastano, H., Jr., John, V. M., Agopyan, V., & Moslemi, A. (2010). Special issue on inorganic-bonded fiber composites. *Construction & Building Materials*, *24*(2), 129–220.

Schadler, L. S., Kuar, S. K., Benicewicz, B. C., Lewis, S. L., & Harton, S. E. (2007). Designed interfaces in polymer nanocomposites: A fundamental viewpoint. *Materials Research Society Bulletin*, *2*, 335–340.

Schaefer, D. W., & Justice, R. S. (2007). How nano are nanocomposites. *Macromolecules*, *40*, 8501–8517.

Shi, J., Lu, L., Guo, W., Zhang, J., & Cao, Y. (2013). Heat insulation performance, mechanics and hydrophobic modification of cellulose–SiO_2 composite aerogels. *Carbohydrate Polymers*, *98*, 282–289.

Sinha, E., & Rout, S. K. (2008). Influence of fibre-surface treatment on structural, thermal and mechanical properties of jute. *Journal of Materials Science*, *43*(8), 2590–2601.

Skreekumar, P. A., Kuruvilla, J., Unnikrishnan, G., & Sabu, T. (2011). Surface-modified sisal fiber-reinforced eco-friendly composites: Mechanical, thermal and diffusion studies. *Polymer Composite*, *32*(1), 131–138.

Tonoli, G. H. D., Rodrigues Filho, U. P., Savastano, H., Jr., Bras, J., Belgacem, M. N., & Rocco Lahr, F. A. (2009). Cellulose modified fibres in cement based composites. *Composites: Part A*, *40*, 2046–2053.

Tonoli, G. H. D., Teixeira, E. M., Corrêa, A. C., Marconcini, J. M., Caixeta, L. A., Pereira-da-Silva, M. A., et al. (2012). Cellulose micro/nanofibres from Eucalyptus Kraft pulp: Preparation and properties. *Carbohydrate Polymers*, *89*, 80–88.

Tonoli, G. H. D., Belgacem, M. N., Siqueira, G., Bras, J., Savastano, H., Jr., & Lahr, F. A. R. (2013). Processing and dimensional changes of cement based composites reinforced with surface-treated cellulose fibres. *Cement and Concrete Composites*, *37*, 68–75.

Tripathi, B. P., & Shahi, V. K. (2011). Organic–inorganic nanocomposite polymer electrolyte membranes for fuel cell applications. *Progress in Polymer Science*, *36*, 945–979.

Xie, K., Yu, Y., & Shi, Y. (2009). Synthesis and characterization of cellulose/silica hybrid materials with chemical crosslinking. *Carbohydrate Polymers*, *78*, 799–805.

Yildiz, S., & Gumuskaya, E. (2007). The effect of thermal modification on crystalline structure of cellulose in soft and hardwood. *Building and Environmental*, *42*, 62–67.